The elaborate route for UDP-arabinose delivery into the Golgi of plants

Carsten Rautengarten[a,b], Devon Birdseye[b], Sivakumar Pattathil[c,1], Heather E. McFarlane[a], Susana Saez-Aguayo[d], Ariel Orellana[d], Staffan Persson[a], Michael G. Hahn[c], Henrik V. Scheller[b,e], Joshua L. Heazlewood[a,b], and Berit Ebert[a,b,2]

[a]School of BioSciences, The University of Melbourne, Melbourne, VIC 3010, Australia; [b]Joint BioEnergy Institute, Biological Systems and Engineering Division, Lawrence Berkeley National Laboratory, Berkeley, CA 94702; [c]Complex Carbohydrate Research Center, University of Georgia, Athens, GA 30602; [d]Centro de Biotecnología Vegetal, Fondo de Areas Prioritarias Center for Genome Regulation, Facultad de Ciencias Biológicas, Universidad Andrés Bello, Santiago RM 8370146, Chile; and [e]Department of Plant and Microbial Biology, University of California, Berkeley, CA 94720

Edited by Natasha V. Raikhel, Center for Plant Cell Biology, Riverside, CA, and approved March 9, 2017 (received for review February 5, 2017)

In plants, L-arabinose (Ara) is a key component of cell wall polymers, glycoproteins, as well as flavonoids, and signaling peptides. Whereas the majority of Ara found in plant glycans occurs as a furanose ring (Ara*f*), the activated precursor has a pyranose ring configuration (UDP-Ara*p*). The biosynthesis of UDP-Ara*p* mainly occurs via the epimerization of UDP-xylose (UDP-Xyl) in the Golgi lumen. Given that the predominant Ara form found in plants is Ara*f*, UDP-Ara*p* must exit the Golgi to be interconverted into UDP-Ara*f* by UDP-Ara mutases that are located outside on the cytosolic surface of the Golgi. Subsequently, UDP-Ara*f* must be transported back into the lumen. This step is vital because glycosyltransferases, the enzymes mediating the glycosylation reactions, are located within the Golgi lumen, and UDP-Ara*p*, synthesized within the Golgi, is not their preferred substrate. Thus, the transport of UDP-Ara*f* into the Golgi is a prerequisite. Although this step is critical for cell wall biosynthesis and the glycosylation of proteins and signaling peptides, the identification of these transporters has remained elusive. In this study, we present data demonstrating the identification and characterization of a family of Golgi-localized UDP-Ara*f* transporters in *Arabidopsis*. The application of a proteoliposome-based transport assay revealed that four members of the nucleotide sugar transporter (NST) family can efficiently transport UDP-Ara*f* in vitro. Subsequent analysis of mutant lines affected in the function of these NSTs confirmed their role as UDP-Ara*f* transporters in vivo.

Golgi apparatus | nucleotide sugars | membrane transport | arabinose

The monosaccharide L-arabinose (Ara) is the second most abundant pentose found in plants and comprises between 10% and 20% of the noncellulosic polysaccharide fraction of *Arabidopsis* leaves (1). It is a key component of the pectic wall polymer rhamnogalacturonan-I (RG-I) as well as being found in hydroxyproline-rich glycoproteins (HRGPs) such as arabinogalactan proteins (AGPs) and extensins (2, 3). Both, RG-I and AGPs, share similar Ara-containing structures, which comprise galactan chains substituted with terminal Ara, and possess relatively large quantities of Ara in the form of α-1,5-linked and -branched arabinan (4, 5). Single Ara residues are also present in the complex pectic polymer rhamnogalacturonan-II (RG-II) (6). In grasses, the majority of Ara is found in arabinoxylan, where it occurs as a decoration of the xylan backbone (7). In dicots, such as *Arabidopsis*, xylan is less frequently arabinosylated. However, recently it was shown that an *Arabidopsis* AGP is covalently linked to pectin and arabinoxylan (8). Ara is also found in xyloglucans of some plant species (9). The XXGG-type xyloglucan found in Solanaceous species is characterized by branches extended with Ara instead of D-galactose (Gal) (10). Ara residues are also critical for signaling processes because mature signaling peptides such as CLAVATA3 require posttranslational arabinosylation in the Golgi apparatus to be biologically active and bind to their receptors (11). In addition to the occurrence of Ara in cell wall polysaccharides, glycoproteins, and secreted peptides, which are made in the Golgi lumen, it is also found in the cytosol-biosynthesized flavonoids such as quercetin glycoside (12) and myricetin glycoside (13).

Ara occurs in two different ring forms, the furanose and the pyranose form. With few exceptions, for example, Ara found in RG-II sidechain B (6), the majority of Ara found in plants, occurs in the furanose form (Ara*f*). This fact is somewhat surprising because in solution, Ara mainly exists in the more stable pyranose form (Ara*p*). Likewise, the nucleotide sugar donor precursor for the biosynthesis of Ara-containing wall glycans is formed as a pyranose ring (UDP-Ara*p*) via two different pathways. UDP-Ara*p* can be formed either de novo by 4-epimerization of UDP-xylose (UDP-Xyl) in the Golgi lumen or via the Ara salvage pathway in the cytosol (14–16). Like most UDP sugars, most UDP-Ara*p* is generated de novo in a sequential conversion from UDP-glucose (UDP-Glc), and subsequently via UDP-glucuronic acid (UDP-GlcA) and UDP-Xyl. The final interconversion step from UDP-Xyl to UDP-Ara*p* is catalyzed by the UDP-Xyl 4-epimerase (UXE1). The *Arabidopsis* mutant *murus4* (*mur4*), which was identified in a mutant screen, affects UXE1 activity (17) and has reduced amounts of cell wall Ara. UXE1 is localized within the Golgi and its catalytic domain is predicted to occur in the lumen (14). Thus, UDP-Ara*p* synthesized via the luminal interconversion pathway provides the substrate for glycosylation reactions requiring UDP-Ara*p*. Whereas it has

Significance

Nucleotide sugars, the activated sugar donors essential for processes such as cell wall biosynthesis and protein and lipid glycosylation are predominantly made in the cytosol. However, a highly diverse range of glycosyltransferases that are located within the Golgi lumen, mediate the above-mentioned glycosylation reactions. Thus, transport of nucleotide sugars across the Golgi membrane into the lumen is crucial for growth and development of many species including microorganisms, plants, and humans. In this study, we identify and functionally characterize four UDP-arabinofuranose transporters from *Arabidopsis* that are responsible for the delivery of activated arabinose, a critical sugar of plant cell walls, glycoproteins, and signaling peptides.

Author contributions: C.R., H.V.S., J.L.H., and B.E. designed research; C.R., D.B., S. Pattathil, H.E.M., S.S.-A., and B.E. performed research; C.R. contributed new reagents/analytic tools; C.R., S. Pattathil, H.E.M., A.O., S. Persson, M.G.H., H.V.S., J.L.H., and B.E. analyzed data; and C.R., J.L.H., and B.E. wrote the paper.

The authors declare no conflict of interest.

This article is a PNAS Direct Submission.

Freely available online through the PNAS open access option.

[1]Present address: Mascoma LLC (Lallemand, Inc.), Lebanon, NH 03766.

[2]To whom correspondence should be addressed. Email: berit.ebert@unimelb.edu.au.

This article contains supporting information online at www.pnas.org/lookup/suppl/doi:10.1073/pnas.1701894114/-/DCSupplemental.

been demonstrated that the cytosolic UDP-glucose 4-epimerases UGE1 and UGE3 can also catalyze the C-4 epimerization of UDP-Xyl to UDP-Ara*p* in vitro (16), the *uge1uge3* double mutant does not show any reduction in cell wall Ara content (18). Thus, a significant de novo interconversion pathway in the cytosol, generating UDP-Ara*p* for Ara-containing polysaccharides assembled in the Golgi apparatus, is unlikely. Besides these de novo pathways, UDP-Ara*p* can also be generated in the cytosol from free Ara released during degradation and metabolism of Ara-containing compounds and polymers. The Ara salvage pathway involves the sequential action of the substrate-specific arabinokinase I (19) and a UDP-sugar pyrophosphorylase with broad substrate specificity (15, 16). Given that the predominant form of Ara found in plants is Ara*f*, UDP-Ara*p* must be interconverted to UDP-Ara*f* before polymer incorporation. The mutase responsible for this reaction was first identified in rice (20). In *Arabidopsis*, this reaction is catalyzed by at least three UDP-Ara mutases [reversibly glycosylated polypeptides (RGPs)], which have been shown to function in the cytosol, although they seem to be associated with the cytosolic side of the Golgi membrane (1). The UDP-Ara*f* synthesized in the cytosol requires transport back into the lumen of the Golgi apparatus. This step is crucial, because the glycosyltransferases (GTs), the group of enzymes that mediate the biosynthesis of glycans for cell wall polymers, are located within this compartment (21) and the pyranose form, synthesized in the Golgi apparatus, is not the preferred donor substrate. Therefore, to enable the biosynthesis of Ara*f*-containing wall polymers, transport of UDP-Ara*f* from the cytosol into the lumen is essential (Fig. S1).

In plants, a family of NSTs has evolved to enable the transport of nucleotide sugars from the cytosol into the Golgi lumen. The *Arabidopsis* NST family contains 51 members falling into six subclades as part of the NST/triose phosphate translocator (TPT) superfamily (22). Some *Arabidopsis* NSTs localized in the Golgi and/or endoplasmic reticulum (ER) that transport GDP-mannose, UDP-galactose, UDP-glucose, UDP–*N*-acetylgalactosamine, and UDP–*N*-acetylglucosamine have been reported in the past decade (23). Recently, a robust assay to determine nucleotide sugar transport activities has been developed and enabled the characterization of the bifunctional UDP-rhamnose/UDP-galactose transporter family, the UDP-Xyl transporter family, the GDP-fucose transporter, and a UDP-uronic acid transporter (22, 24–26).

Whereas the compartmentalization of UDP-Ara interconverting mutases and GTs requiring UDP-Ara*f* as activated donor substrate clearly argues for the existence of an UDP-Ara*f* transporter, no such NST has yet been identified. Here, we report the characterization of the UDP-Ara*f* transporter (UAfT) family from *Arabidopsis*. Using a refined transporter assay in conjunction with detection by mass spectrometry, we show that four members constituting the UAfT family are capable of efficiently transporting UDP-Ara*f*. Analysis of the subcellular localization indicates that all four members are present in the Golgi apparatus supporting their function as Golgi UDP-Ara*f* transporters. An examination of plant lines overexpressing UDP-Ara*f* transporter candidates confirmed an in vivo function as UDP-Ara*f* transporters.

Results

Members of Clade VI of the NST Family Transport UDP-Ara*f*. A substrate screen conducted on the entire *Arabidopsis* NST family identified members of clade VI subclade A (AT5G25400, AT5G11230, AT4G32390, and AT2G25520) and subclade B (AT3G17430 and AT1G48230) (Fig. S2) with specificities for UDP-Ara*f* when proteoliposomes were preloaded with UMP. Each of these NSTs was heterologously expressed in yeast and its presence in microsomal preparations was assessed by immunoblotting (Fig. 1*A*). The ability of each NST to transport nucleotide sugar substrates was assessed by LC-MS/MS after conducting the transport assay with 16 nucleotide/nucleotide sugar substrates (listed in Table S1) against each of the putative exchange

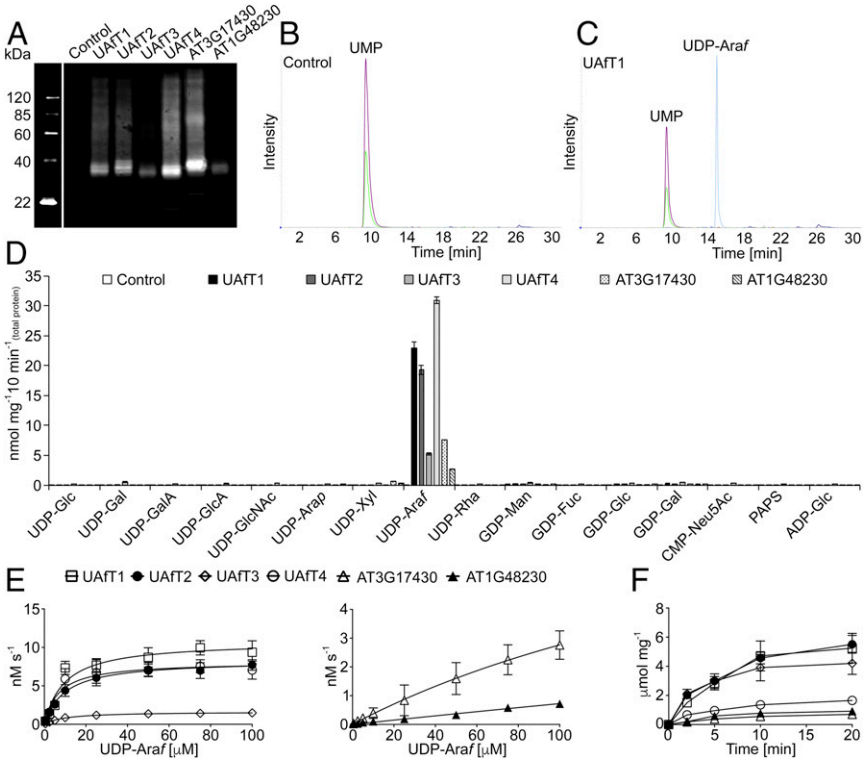

Fig. 1. Determining the substrate specificity and kinetics of UAfT candidates. (*A*) Immunoblot analysis of microsomes isolated from yeast transformed with the empty vector (control), UAfT1–4, AT3G17430, and AT1G48230 (2.5 μg protein per lane). (*B*) Representative MRM analysis of proteoliposomes preloaded with 10 mM UMP generated from a control after conducting the transport assay with 16 nucleotide sugar substrates. (*C*) Representative MRM analysis of UAfT1-containing proteoliposomes preloaded with 10 mM UMP after conducting the transport assay with 16 nucleotide sugar substrates. (*D*) Quantification of nucleotide sugar transport into proteoliposomes preloaded with 10 mM UMP after incubation with 16 nucleotide sugar substrates. Data are the mean and SD of $n = 4$ assays. (*E*) Proteoliposomes containing each candidate preloaded with 10 mM UMP were incubated with UDP-Ara*f* at varying concentration (0.5–100 μM) for 2 min at 25 °C. Data are the mean and SEM of $n = 8$ assays. (*F*) Proteoliposomes containing each candidate preloaded with 10 mM UMP were incubated with UDP-Ara*f* at a concentration of 50 μM for the indicated time points at 25 °C. Values are normalized to the calculated NST content present in proteoliposome preparations. Data are the mean and SD of $n = 8$ assays. Legend as shown in *E* applies.

substrates UMP, GMP, CMP, or AMP. An empty vector control was used to assess background transport after removal of unincorporated substrates by gel filtration (Fig. 1*B*). A typical output after a single transport assay using proteoliposomes containing AT5G25400 preloaded with UMP is outlined in Fig. 1*C*. All six NST candidates demonstrated significant transport of UDP-Ara*f* when proteoliposomes were preloaded with UMP (Fig. 1*D*). No apparent transport was observed when proteoliposomes were preloaded with GMP, CMP, or AMP. The observed GDP-sugar transport when proteoliposomes were preloaded with GMP can be accounted for by activity of the endogenous yeast GDP-Man transporter (Fig. S3).

Kinetic Parameters of UDP-Ara*f* Transport. The transport response of each NST candidate to UDP-Ara*f* was then independently determined. Subclade A members appeared to be saturable in a concentration-dependent manner, as would be expected for protein-mediated transport across a membrane (Fig. 1*E*). In contrast, the two subclade B members did not show saturation with substrate concentrations up to 100 μM (Fig. 1*E*). All six NST candidates were saturable in a time-dependent manner (Fig. 1*F*). Analysis of these data resulted in apparent K_Ms for UDP-Ara*f* for members of subclade A, ranging from 7 to 10 μM with resultant turnover rates (k_{cat}) of 1–4 s^{-1} (Table 1). We were unable to obtain corresponding kinetic parameters for members of subclade B. Consequently, the four members of the *Arabidopsis* NST clade VI, subclade A were designated the functional identifier **U**DP-**A**rabino**f**uranose **T**ransporters (UAfT), and comprise the *Arabidopsis* loci AT5G25400 (*UAfT1*), AT5G11230 (*UAfT2*), AT4G32390 (*UAfT3*), and AT2G25520 (*UAfT4*). Previously, we have compared the apparent K_M with the physiological concentrations of the substrate in plant organs to support the in vitro kinetic values (22, 24). The concentration of UDP-Ara*f* in various plant organs was determined to be in the range of 5–15 pmol mg^{-1} dry weight (22). Because UDP-Ara*f* is synthesized within the cytosol (1), we have previously reasoned that given that the vacuole generally comprises the bulk of a plant cells volume, dry weight measurements would be somewhat analogous to the volume of the cell excluding the vacuole. Consequently, an estimate for the cellular concentrations of UDP-Ara*f* within the plant cell would be between 5 and 15 μM. This physiological concentration range aligns well with the determined K_M values outlined above and supports the notion that we have identified biologically relevant transporters.

Developmental Expression and Subcellular Localization. The expression patterns for the *UAfTs* were analyzed from a variety of organs using quantitative RT-PCR (qPCR) (Fig. 2*A*). All four members are expressed throughout plant development, although they are disproportionally expressed in flowers and during seed development (siliques), which are rich in Ara-containing polysaccharides. The expression patterns agree with those observed in publicly available microarray expression data (27). The subcellular locations were determined by transiently expressing C-terminal yellow fluorescent protein (YFP) fusions in *Nicotiana benthamiana* leaves and colocalizing the signal with the α-ManI mCherry Golgi-marker (G-rk) and a mCherry ER marker (ER-rk) (Fig. 2*B*). Simultaneous dual-channel live-cell imaging revealed localization of all UAfT–YFP fusions in the endomembrane system and resulted in punctate signals that highly colocalized with the Golgi marker. Subcellular proteome studies have identified all UAfTs, except for UAfT1, in the Golgi apparatus (28), supporting their roles as Golgi-localized UDP-Ara*f* transporters.

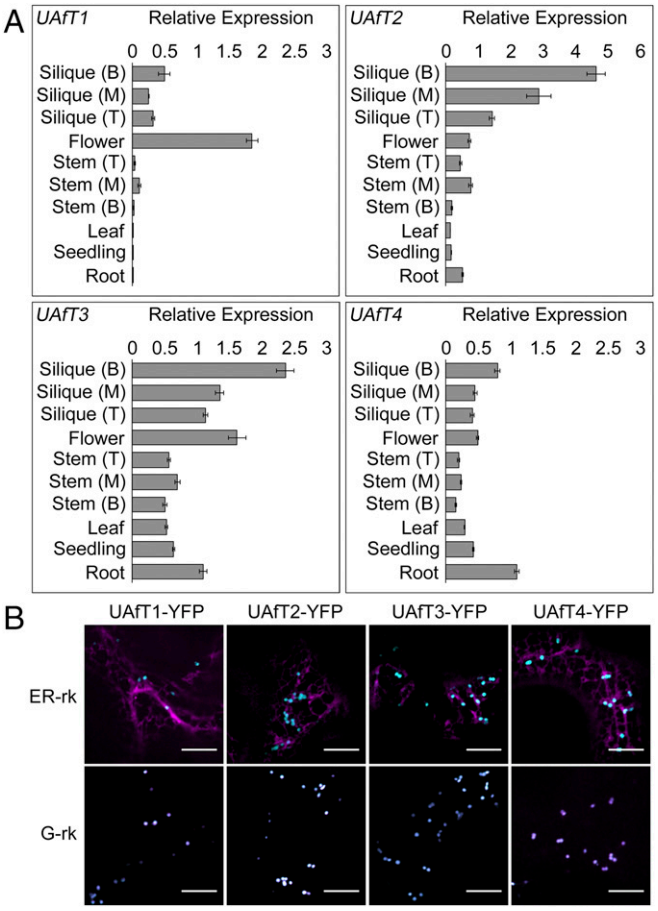

Fig. 2. Expression pattern and subcellular localizations. (*A*) Expression of *UAfTs* in different *Arabidopsis* organs was assessed by qPCR. Siliques and stem tissues were harvested from the bottom (B), middle (M) and top (T). Expression levels are the mean and SD of $n = 3$ expressed relative to three reference genes. (*B*) UAfTs were transiently coexpressed with the α-mannosidase I Golgi marker (G-rk) or the ER marker (ER-rk) in *N. benthamiana* leaves. All four UAfTs colocalize with the Golgi marker. (Scale bars, 10 μm.)

Table 1. Kinetic parameters for UDP-Ara*f* transport into proteoliposomes

Parameter	UAfT1	UAfT2	UAfT3	UAfT4	AT3G17430	AT1G48230
K_M (μM)	10 (1)	10 (1)	10 (2)	7 (1)	Ambiguous	Ambiguous
V_{max} (nM s^{-1})	11 (0)	8 (0)	2 (0)	8 (0)	N.D.	N.D.
k_{cat} (s^{-1})	4	3	3	1	N.D.	N.D.

For each transporter, eight data points with varying substrate concentrations (0.5–100 μM) were acquired. Data represent the mean and SEM of $n = 8$ replicates. N.D., not determined.

Determining in Planta Functions of UAfTs. To confirm the in vitro biochemical characterization of the UAfTs, we obtained *Arabidopsis* mutant lines for each of the four members. For both, *UAfT2* and *UAfT3*, we could confirm two independent knockout lines; for *UAfT4* a knockout and knockdown line were verified and for *UAfT1* only a single knockout line could be identified (Fig. S4). The analysis of homozygous *UAfT* knockout lines grown under standard growth conditions did not reveal any morphological alterations compared with wild-type plants. Cell wall preparations derived from leaves of 6-wk-old plants revealed a minor but significant reduction in Ara in both *uaft4* lines (Table S2). Given the higher expression levels of *UAfT2* and *-3* in siliques (Fig. 2*A*) and of *UAfT2*, *-3*, and *-4* in developing embryos (29), we sought to also analyze the cell wall monosaccharide composition of dry

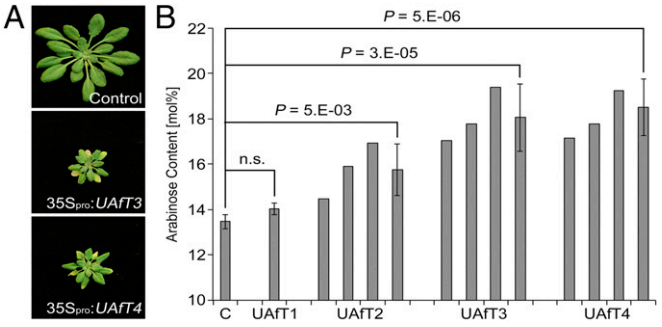

Fig. 3. Overexpression of UAfTs result in morphological and biochemical phenotypes. (*A*) Representative phenotypes of plants overexpressing UAfT3 or UAfT4 compared with a control plant. (*B*) Arabinose content of rosette leaves. Three biological pools corresponding to the severity of the phenotype were analyzed. Arabinose levels are shown as molar percentage of total nonglucan carbohydrates ± SD ($n = 3$).

seeds derived from the corresponding knockout lines. As observed for leaf material, no major change in the abundance of monosaccharides was observed in dry seeds from these plants (Table S3). These results indicate that, at the examined resolution, some of the four UAfTs might function redundantly in *Arabidopsis*. Redundancy between NST family members in *Arabidopsis* seems to be relatively common (22), and we have previously found that the generation of NST overexpression (OE) lines results in attributable phenotypes. Consequently, we stably expressed the four *UAfTs* under the control of the CaMV 35S promoter and fused to YFP in *Arabidopsis*. For plants transformed with the $35S_{pro}$:*UAfT1*–YFP construct, YFP florescence could not be observed, indicating that this transgene had likely been silenced. For plants harboring the $35S_{pro}$:*UAfT3–YFP* or $35S_{pro}$:*UAfT4–YFP* constructs, we observed that lines possessing a strong YFP signal were retarded in their growth and showed early yellowing of leaves (Fig. 3*A*). An analysis of the monosaccharide content of leaf cell wall material indicated that UAfT2, -3, and -4 OE plant lines all contained a significant increase in the amounts of Ara (Fig. 3*B*). In particular, the overexpression of UAfT3 and UAfT4 led to a strong accumulation of Ara (up to 30% more compared with control plants) and concomitantly resulted in obvious phenotypic abnormalities (Fig. 3*A*). This result was observed predominantly for UAfT3 and UAfT4 OE lines, but only occasionally for UAfT2 overexpressors.

Glycome Profiling of UAfT3 and UAfT4 Overexpression Lines. To investigate where the additional Ara in plants overexpressing UAfT3 or UAfT4 was incorporated, we performed glycome profiling using an ELISA-based screen with a collection of 155 plant cell wall glycan-directed monoclonal antibodies (30). Interestingly, the glycome profiles of wall extracts from UAfT3 and UAfT4 OE lines were different (Fig. 4). The most pronounced differences between UAfT3 OE lines and the control were observed in water-soluble cell wall material, particularly for antibodies recognizing arabinogalactan epitopes in RG-I and AGPs (RG-I/AG and AG-4 antibody groups). In contrast, the most pronounced differences between cell wall extracts from UAfT4 OE lines and control plants were observed in the sodium carbonate extracts (enriched for pectic polymers). Similar to the results observed for UAfT3 OE lines, the difference in the recognition pattern between the control and UAfT4 OE lines was predominantly due to antibodies recognizing pectic backbones, such as JIM5, which recognizes homogalacturonan (31), or CCRC-M36, which is specific for the RG-I backbone (32), or arabinogalactan epitopes in RG-I and AGP (RG-I/AG and AG-4). The observation that the UAfT3 and UAfT4 OE lines vary between different extracts is further supported by the data for the LM6 antibody, which is specific to 1,5-α-arabinan (33). An increased signal for LM6 was observed in the water-extracted material derived from UAfT3 OE plants, whereas the increase in binding intensity in UAfT4 OE lines is clearly visible in the sodium carbonate extract. Water-soluble extracts of UAfT4 OE lines showed stronger binding to acetylated glucomannan-directed antibodies than that observed for the UAfT3 OE or control lines. The 4 N KOH extracts (enriching hemicelluloses) showed decreased binding by LM5, which is specific for a β-1,4-galactan epitope (34) and could indicate that an increase in arabinose content leads to increased 1,5-α-arabinan decoration

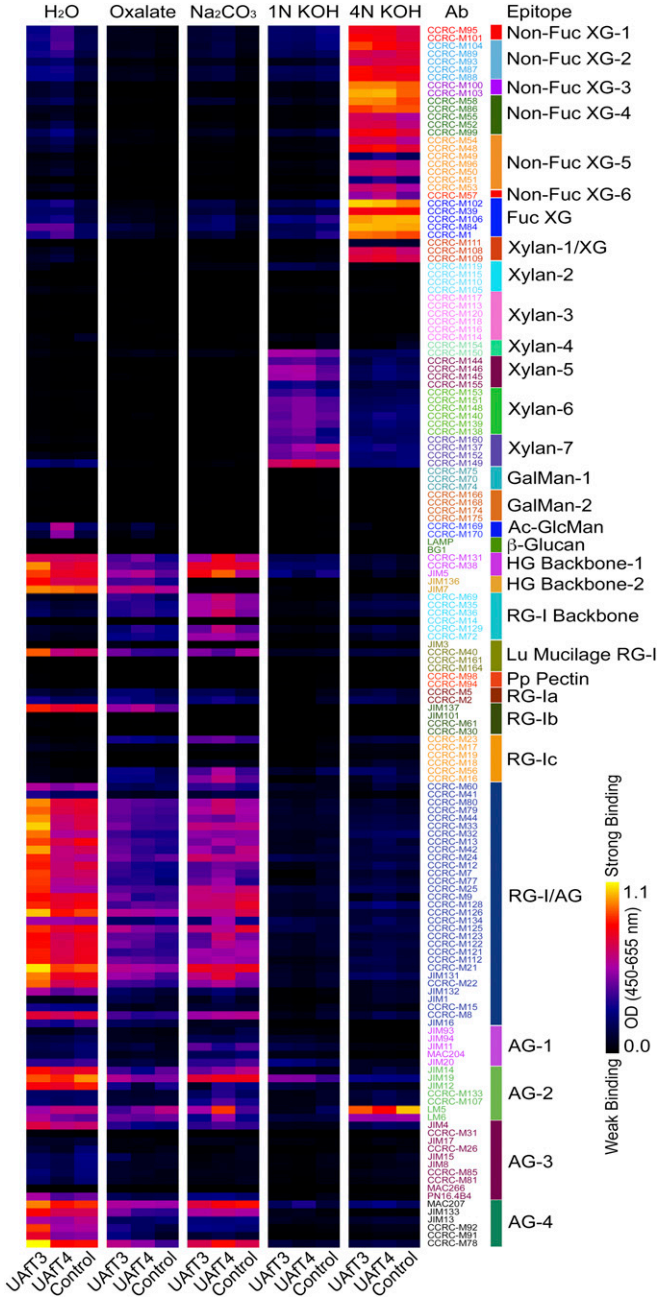

Fig. 4. Glycome profiling. Sequentially extracted cell wall material derived from plants overexpressing UAfT3, UAfT4, and control plants was subjected to glycome profiling using 155 plant cell wall glycan-directed monoclonal antibodies. A black–yellow scale indicates signal intensity in the ELISA, with black corresponding to no binding and yellow to strongest binding. Labels at the *Top* specify the different reagents used to extract the cell wall material.

and consequently reduced unsubstituted galactan epitopes in RG-I in the OE lines. Antibodies belonging to the groups of non-fucosylated and fucosylated xyloglucan also show subtle differences in their binding to wall extracts between the control and both the UAfT3 and UAfT4 OE lines. Another interesting difference was the marginal increase in the abundances of 1 N KOH extractable xylan epitopes (especially epitopes recognized by xylan-4 through xylan-6 groups of antibodies) in the two OE lines.

Discussion

The ubiquitous presence of Ara in an assortment of cell wall-associated polymers, its presence in flavonoids, and its association with signaling molecules highlight the important role of this monosaccharide as both a structural component of walls and in regulating growth and development. The majority of Ara is found in cell wall-associated polymers where it is mainly present in its furanose form. Whereas luminal nucleotide sugar interconversion results in the biosynthesis of an activated Ara donor, it is in the pyranose form. The characterization of the UDP-Ara mutases and their localization to the cytosol resulted in a biosynthetic dilemma, because UDP-Ara*f* is required within the Golgi lumen necessary for the biosynthesis of cell wall-associated polysaccharides. The characterization of a family of four *Arabidopsis* NSTs with substrate specificity for UDP-Ara*f* reveals the final step in the delivery pathway for Ara*f*-containing compounds synthesized in the lumen and supports the current biosynthetic model of nucleotide sugar interconversion (Fig. S1).

The Partitioning of UDP-Ara Within the Plant Cell. The biosynthesis of Ara-containing compounds within the Golgi requires UDP-Ara be transported twice across the Golgi membrane. A likely explanation for this process is the thermodynamic equilibrium of UDP-Ara*f* biosynthesis by the UDP-Ara mutases. The in vitro characterization of those enzymes from either rice or *Arabidopsis* indicates that only about 10% of UDP-Ara*p* is converted to UDP-Ara*f* (1, 35). This inefficient conversion is a probable reason for the partitioning of UDP-Ara*f* biosynthesis in the cytosol and its incorporation within the Golgi lumen, enabling the efficient and noncompetitive transfer of Ara*f* to a nucleophilic acceptor. The ability to modify the composition of Ara in cell wall-associated material through the up-regulation of UAfTs indicates that the supply of UDP-Ara*f* within the Golgi lumen is likely limiting. The increased availability of this nucleotide sugar within the Golgi and resultant increase in Ara in the cell wall also provides information about the distribution of UDP-Ara*f* and UDP-Ara*p* within the cell. We previously determined that the amount of UDP-Ara*p* within a variety of *Arabidopsis* organs is 40–105 pmol mg^{-1} dry weight, whereas the amount of UDP-Ara*f* ranges from 5 to 15 pmol mg^{-1} dry weight (22). Considering the thermodynamic equilibrium of UDP-Ara mutases with these concentrations and given the limited availability of UDP-Ara*f* for incorporation into luminal polysaccharides, it is likely that the biochemical pools of both UDP-Ara*p* and UDP-Ara*f* exist predominantly within the cytosol, even with the former actively made by the Golgi-resident UDP-Xyl 4-epimerase 1 (UXE1). The location of UDP-Ara*f* in the cytosol is supported by the investigation of a GT47 family member, ARABINAN DEFICIENT 1 (ARAD1), which is implicated in pectic arabinan biosynthesis (36). Plants overexpressing ARAD1 did not show an altered arabinan content (36), potentially indicating limitations in substrate availability (37). In contrast, evidence for a distinct cytosolic pool of UDP-Ara*p* is supported by the recently characterized Golgi-resident UDP-xylose transporters (UXTs) and their role in xylan biosynthesis (24) as well as the fact that the Golgi-localized UDP-xylose synthases (UXS) have a limited role in supplying substrates for xylose-containing polymers within the Golgi lumen (38). Both findings indicate that the fate of luminal synthesized UDP-Xyl is mainly to provide the substrate for UXE1 for the biosynthesis of UDP-Ara*p*. This latter observation is supported by a UXS triple mutant in *Arabidopsis* (*uxs3uxs5uxs6*) that eliminated cytosolic-derived UDP-Xyl (38), and resulted in an increased Ara content in cell wall extracts. The removal of the cytosolic UDP-Xyl pool likely results in an increased flux through the luminal interconversion pathway, driving the biosynthesis of UDP-Ara*p* thus explaining the increased levels of Ara. Moreover, because the reported equilibrium between UDP-Xyl and UDP-Ara*p* by UXE1 is around 1:1 (14), the transport of UDP-Ara*p* outside of the Golgi (by an unidentified NST) would provide the necessary pull on the luminal interconversion pathway to ensure sufficient supply of UDP-Ara*f* for luminal polysaccharide biosynthesis. This model is also supported by studies on the *mur4* mutant and wild-type plants, where the addition of exogenous Ara increased polysaccharide arabinosylation (17), supporting a limited delivery of UDP-Ara*f* into the Golgi lumen.

The Role of Ara in the Plant Cell Wall. Ara comprises a significant proportion of the plants cell wall. In *Arabidopsis*, the modulation of Ara quantity results in a severe growth phenotype. Both UAfT3 and UAfT4 OE lines displayed up to ∼30% increase in Ara content in cell wall extracts, which correlated with reduced growth and early senescing leaves (Fig. 3*A*). Glycome profiling indicated that epitopes corresponding to RG-I, RG-I-associated arabinogalactans, and AGPs increased in both UAfT3 and UAfT4 OE lines. Similarly, cytosolic UXS triple mutant plants (*uxs3uxs5uxs6*), which likely result in an increased flux through the luminal interconversion pathway, contain a twofold increase in cell wall-derived Ara and display a reduced growth phenotype (38). Analysis of stem wall material from the *uxs3uxs5uxs6* triple mutant indicated that increased Ara was mainly present as 1,5-Ara(*f*) linkage and represents an increase in length or quantity of α-1,5-arabinan sidechains in the pectic polymer RG-I. Thus, the increased Ara content observed here can likely be attributed to increases in RG-I arabinan.

It has been speculated that RG-I sidechains act as spacers and regulate interactions with homogalacturonan, thus controlling the flexibility of the cell wall (39). The plasticity of the wall relies on the mobility of RG-I sidechains, especially arabinan (40), and the modulation of sidechain lengths and branching seems to have a deleterious effect on the physical properties of the wall. Such conclusions have been made examining transgenic potato plants expressing a Golgi-localized α-1,5-arabinanase (41). This contrasts with modulations to the galactan sidechains of RG-I because plants overexpressing the galactan synthase GALS1 or the UDP-Gal/UDP-Rha transporter URGT1 contain up to 50% more cell wall galactose specifically in the form of pectic β-1,4-galactan but plant growth and development are not affected (22, 42). These contrasting observations highlight the special importance of arabinan sidechains for proper RG-I function.

Conclusion

Ara plays an essential role in the growth and development of plants. Here we have characterized a family of Golgi nucleotide sugar transporters (UAfTs) responsible for the delivery of UDP-Ara*f* for a range of Golgi luminal arabinosylation reactions in *Arabidopsis*. This study represents the only example of UDP-Ara*f* transport in biology and the characterization of this family supports the curious model for the incorporation of UDP-Ara*f* in plants.

Materials and Methods

Nucleotide Sugar Substrates. Nucleotide/nucleotide sugar substrates used in this study are listed in Table S1. UDP-β–L-rhamnose and GDP-α–L-galactose were synthesized enzymatically as previously described (22).

Heterologous Expression of NSTs in Yeast and Transport Assays. Heterologous expression was undertaken in *Saccharomyces cerevisiae* strain INVSc1 using the expression vector pYES-DEST52 (Thermo Fisher Scientific). Reconstitution of NSTs and transport activity assays were conducted as previously described (22). Kinetic parameters were determined using nonlinear regression with Prism 7 software (GraphPad Software). Polyacrylamide gel electrophoreses and immunoblot analyses were carried out as previously described (22).

Analysis of Nucleotide Sugars by Tandem Mass Spectrometry. Nucleotide sugars were separated on a Hypercarb porous graphitic carbon column (Thermo Fisher Scientific) with a 1100 series HPLC system (Agilent Technologies) and analyzed by LC-MS/MS and multiple reaction monitoring (MRM) using a 4000 QTRAP system (Sciex) with conditions and parameters as previously outlined (22).

Plant Material. *A. thaliana* seeds were acquired from the *Arabidopsis* Biological Resource Center (*SI Materials and Methods*).

Fractionation of Cell Wall Material and Glycome Profiling. Glycome profiling was performed with a comprehensive suite of plant cell wall glycan-directed monoclonal antibodies (30) as described (43) (*SI Materials and Methods*).

ACKNOWLEDGMENTS. J.L.H., B.E., and S. Persson are supported by Australian Research Council (ARC) Future Fellowships (FT130101165, FT160100276, and FT160100218). H.E.M. is supported by an ARC Discovery Early Career Researcher Award (DE170100054). Microscopy was supported by an ARC Linkage Infrastructure, Equipment, and Facilities (LE150100011) and Biological Optical Microscopy Platform (The University of Melbourne). The work was supported by the US Department of Energy through contract DE-AC02-05CH11231 with Lawrence Berkeley National Laboratory and contract DE-AC05-00OR22725 with Oak Ridge National Laboratory. A.O. is supported by Fondecyt 1151335, Fondo de Areas Prioritarias-Centro de Regulacion del Genoma 15090007, Committee of Evaluation and Direction of the Scientific Cooperation-CONICYT C14B02, and Basal Program PB-16. S.S.-A. is supported by Fondecyt 11160787. The generation of the Complex Carbohydrate Research Center series of plant cell wall glycan-directed antibodies was supported by the NSF Plant Genome Program (DBI-0421683 and IOS-0923992). Substrates from CarboSource Services (Athens, GA) were supported by NSF-Research Coordination Networks Grant 0090281.

1. Rautengarten C, et al. (2011) The interconversion of UDP-arabinopyranose and UDP-arabinofuranose is indispensable for plant development in Arabidopsis. *Plant Cell* 23: 1373–1390.
2. Bar-Peled M, O'Neill MA (2011) Plant nucleotide sugar formation, interconversion, and salvage by sugar recycling. *Annu Rev Plant Biol* 62:127–155.
3. Showalter AM, Basu D (2016) Extensin and arabinogalactan-protein biosynthesis: Glycosyltransferases, research challenges, and biosensors. *Front Plant Sci* 7:814.
4. Seifert GJ, Roberts K (2007) The biology of arabinogalactan proteins. *Annu Rev Plant Biol* 58:137–161.
5. Willats WG, McCartney L, Mackie W, Knox JP (2001) Pectin: Cell biology and prospects for functional analysis. *Plant Mol Biol* 47:9–27.
6. Bar-Peled M, Urbanowicz BR, O'Neill MA (2012) The synthesis and origin of the pectic polysaccharide rhamnogalacturonan II: Insights from nucleotide sugar formation and diversity. *Front Plant Sci* 3:92.
7. Scheller HV, Ulvskov P (2010) Hemicelluloses. *Annu Rev Plant Biol* 61:263–289.
8. Tan L, et al. (2013) An Arabidopsis cell wall proteoglycan consists of pectin and arabinoxylan covalently linked to an arabinogalactan protein. *Plant Cell* 25:270–287.
9. Peña MJ, Darvill AG, Eberhard S, York WS, O'Neill MA (2008) Moss and liverwort xyloglucans contain galacturonic acid and are structurally distinct from the xyloglucans synthesized by hornworts and vascular plants. *Glycobiology* 18:891–904.
10. Schultink A, Cheng K, Park YB, Cosgrove DJ, Pauly M (2013) The identification of two arabinosyltransferases from tomato reveals functional equivalency of xyloglucan side chain substituents. *Plant Physiol* 163:86–94.
11. Ohyama K, Shinohara H, Ogawa-Ohnishi M, Matsubayashi Y (2009) A glycopeptide regulating stem cell fate in *Arabidopsis thaliana*. *Nat Chem Biol* 5:578–580.
12. Halabalaki M, et al. (2011) Quercetin and kaempferol 3-O-[α-L-rhamnopyranosyl-(1→2)-α-L-arabinopyranoside]-7-O-α-L-rhamnopyranosides from Anthyllis hermanniae: Structure determination and conformational studies. *J Nat Prod* 74: 1939–1945.
13. Torres-Mendoza D, et al. (2006) Weakly antimalarial flavonol arabinofuranosides from *Calycolpus warszewiczianus*. *J Nat Prod* 69:826–828.
14. Burget EG, Verma R, Mølhøj M, Reiter WD (2003) The biosynthesis of L-arabinose in plants: Molecular cloning and characterization of a Golgi-localized UDP-D-xylose 4-epimerase encoded by the MUR4 gene of Arabidopsis. *Plant Cell* 15:523–531.
15. Geserick C, Tenhaken R (2013) UDP-sugar pyrophosphorylase is essential for arabinose and xylose recycling, and is required during vegetative and reproductive growth in Arabidopsis. *Plant J* 74:239–247.
16. Kotake T, et al. (2007) Properties and physiological functions of UDP-sugar pyrophosphorylase in Arabidopsis. *Biosci Biotechnol Biochem* 71:761–771.
17. Burget EG, Reiter WD (1999) The *mur4* mutant of arabidopsis is partially defective in the *de novo* synthesis of uridine diphospho L-arabinose. *Plant Physiol* 121:383–389.
18. Rösti J, et al. (2007) UDP-glucose 4-epimerase isoforms UGE2 and UGE4 cooperate in providing UDP-galactose for cell wall biosynthesis and growth of *Arabidopsis thaliana*. *Plant Cell* 19:1565–1579.
19. Dolezal O, Cobbett CS (1991) Arabinose kinase-deficient mutant of *Arabidopsis thaliana*. *Plant Physiol* 96:1255–1260.
20. Konishi T, et al. (2007) A plant mutase that interconverts UDP-arabinofuranose and UDP-arabinopyranose. *Glycobiology* 17:345–354.
21. Oikawa A, Lund CH, Sakuragi Y, Scheller HV (2013) Golgi-localized enzyme complexes for plant cell wall biosynthesis. *Trends Plant Sci* 18:49–58.
22. Rautengarten C, et al. (2014) The Golgi localized bifunctional UDP-rhamnose/UDP-galactose transporter family of Arabidopsis. *Proc Natl Acad Sci USA* 111:11563–11568.
23. Orellana A, Moraga C, Araya M, Moreno A (2016) Overview of nucleotide sugar transporter gene family functions across multiple species. *J Mol Biol* 428:3150–3165.
24. Ebert B, et al. (2015) Identification and characterization of a Golgi-localized UDP-xylose transporter family from Arabidopsis. *Plant Cell* 27:1218–1227.
25. Rautengarten C, et al. (2016) The Arabidopsis Golgi-localized GDP-L-fucose transporter is required for plant development. *Nat Commun* 7:12119.
26. Saez-Aguayo S, et al. (2017) UUAT1 is a Golgi-localized UDP-uronic acid transporter that modulates the polysaccharide composition of Arabidopsis seed mucilage. *Plant Cell* 29:129–143.
27. Schmid M, et al. (2005) A gene expression map of *Arabidopsis thaliana* development. *Nat Genet* 37:501–506.
28. Nikolovski N, et al. (2012) Putative glycosyltransferases and other plant Golgi apparatus proteins are revealed by LOPIT proteomics. *Plant Physiol* 160:1037–1051.
29. Le BH, et al. (2010) Global analysis of gene activity during Arabidopsis seed development and identification of seed-specific transcription factors. *Proc Natl Acad Sci USA* 107:8063–8070.
30. Pattathil S, et al. (2010) A comprehensive toolkit of plant cell wall glycan-directed monoclonal antibodies. *Plant Physiol* 153:514–525.
31. Casero PJ, Knox JP (1995) The monoclonal-antibody Jim5 indicates patterns of pectin deposition in relation to pit fields at the plasma-membrane-face of tomato pericarp cell-walls. *Protoplasma* 188:133–137.
32. Young RE, et al. (2008) Analysis of the Golgi apparatus in Arabidopsis seed coat cells during polarized secretion of pectin-rich mucilage. *Plant Cell* 20:1623–1638.
33. Willats WGT, Marcus SE, Knox JP (1998) Generation of monoclonal antibody specific to (1–>5)-alpha-L-arabinan. *Carbohydr Res* 308:149–152.
34. Jones L, Seymour GB, Knox JP (1997) Localization of pectic galactan in tomato cell walls using a monoclonal antibody specific to (1->4)-beta-D-galactan. *Plant Physiol* 113:1405–1412.
35. Konishi T, et al. (2010) Purification and biochemical characterization of recombinant rice UDP-arabinopyranose mutase generated in insect cells. *Biosci Biotechnol Biochem* 74:191–194.
36. Harholt J, et al. (2006) ARABINAN DEFICIENT 1 is a putative arabinosyltransferase involved in biosynthesis of pectic arabinan in Arabidopsis. *Plant Physiol* 140:49–58.
37. Geshi N, Harholt J, Sakuragi Y, Krüger Jensen J, Scheller HV (2010) *Glycosyltransferases of the GT47 Family. Plant Polysaccharides, Biosynthesis and Bioengineering, Annual Plant Reviews*, ed Ulvskov P (Wiley-Blackwell, New Jersey), Vol 41, pp 265–283.
38. Kuang B, et al. (2016) The role of UDP-glucuronic acid decarboxylase(s) (UXS) in xylan biosynthesis in Arabidopsis. *Mol Plant* 9:1119–1131.
39. Harholt J, Suttangkakul A, Vibe Scheller H (2010) Biosynthesis of pectin. *Plant Physiol* 153:384–395.
40. Ha MA, Viëtor RJ, Jardine GD, Apperley DC, Jarvis MC (2005) Conformation and mobility of the arabinan and galactan side-chains of pectin. *Phytochemistry* 66: 1817–1824.
41. Ulvskov P, et al. (2005) Biophysical consequences of remodeling the neutral side chains of rhamnogalacturonan I in tubers of transgenic potatoes. *Planta* 220:609–620.
42. Liwanag AJ, et al. (2012) Pectin biosynthesis: GALS1 in *Arabidopsis thaliana* is a β-1,4-galactan β-1,4-galactosyltransferase. *Plant Cell* 24:5024–5036.
43. Pattathil S, Avci U, Miller JS, Hahn MG (2012) Immunological approaches to plant cell wall and biomass characterization: Glycome Profiling. *Methods Mol Biol* 908:61–72.
44. Lamesch P, et al. (2012) The Arabidopsis Information Resource (TAIR): Improved gene annotation and new tools. *Nucleic Acids Res* 40:D1202–D1210.
45. Tamura K, Stecher G, Peterson D, Filipski A, Kumar S (2013) MEGA6: Molecular Evolutionary Genetics Analysis version 6.0. *Mol Biol Evol* 30:2725–2729.
46. Schmittgen TD, Livak KJ (2008) Analyzing real-time PCR data by the comparative C(T) method. *Nat Protoc* 3:1101–1108.
47. MacLean B, et al. (2010) Skyline: an open source document editor for creating and analyzing targeted proteomics experiments. *Bioinformatics* 26:966–968.
48. Alonso JM, et al. (2003) Genome-wide insertional mutagenesis of *Arabidopsis thaliana*. *Science* 301:653–657.
49. Woody ST, Austin-Phillips S, Amasino RM, Krysan PJ (2007) The WiscDsLox T-DNA collection: An arabidopsis community resource generated by using an improved high-throughput T-DNA sequencing pipeline. *J Plant Res* 120:157–165.
50. Clough SJ, Bent AF (1998) Floral dip: A simplified method for Agrobacterium-mediated transformation of *Arabidopsis thaliana*. *Plant J* 16:735–743.
51. Earley KW, et al. (2006) Gateway-compatible vectors for plant functional genomics and proteomics. *Plant J* 45:616–629.
52. Nelson BK, Cai X, Nebenführ A (2007) A multicolored set of *in vivo* organelle markers for co-localization studies in Arabidopsis and other plants. *Plant J* 51:1126–1136.
53. Benson DA, Karsch-Mizrachi I, Lipman DJ, Ostell J, Sayers EW (2011) GenBank. *Nucleic Acids Res* 39:D32–D37.